LA-UR-02- 4393

Approved for public release;
distribution is unlimited.

c. 2

Title: ACTIVE PROBING OF CLOUD THICKNESS AND OPTICAL DEPTH USING WIDE-ANGLE IMAGING LIDAR

Author(s): Steven P. Love,
Anthony B. Davis,
Charles A. Rohde,
Larry T. Tellier,
Cheng Ho

Space & Remote Sensing Sciences Group (NIS-2)

Submitted to: Proceedings of
11th AMS Conference on Atmospheric Radiation,
Ogden (Utah), June 3-7, 2002,
AMS, Boston (Ma), ©2002

Los Alamos
NATIONAL LABORATORY

J5.3 ACTIVE PROBING OF CLOUD THICKNESS AND OPTICAL DEPTH USING WIDE-ANGLE IMAGING LIDAR

Steven P. Love,* Anthony B. Davis, Charles A. Rohde, Larry Tellier, Cheng Ho
Space and Remote Sensing Sciences Group (NIS-2), Los Alamos National Laboratory

1. INTRODUCTION AND OVERVIEW

At most optical wavelengths, laser light in a cloud lidar experiment is not absorbed but merely scattered out of the beam, eventually escaping the cloud via multiple scattering. There is much information available in this light scattered far from the input beam, information ignored by traditional "on-beam" lidar. Monitoring these off-beam returns in a fully space- and time-resolved manner is the essence of our unique instrument, Wide Angle Imaging Lidar (WAIL). In effect, WAIL produces wide-field (60° full-angle) "movies" of the scattering process and records the cloud's radiative Green functions. A direct data product of WAIL is the distribution of photon path lengths resulting from multiple scattering in the cloud. Following insights from diffusion theory, we can use the measured Green functions to infer the physical thickness and optical depth of the cloud layer. WAIL is notable in that it is applicable to optically thick clouds, a regime in which traditional lidar is reduced to ceilometry.

Section 2 covers the up-to-date evolution of the nighttime WAIL instrument at LANL. Section 3 reports our progress towards daytime capability for WAIL, an important extension to full diurnal cycle monitoring by means of an ultra-narrow magneto-optic atomic line filter. Section 4 describes briefly how the important cloud properties can be inferred from WAIL signals.

2. EVOLUTION OF WAIL INSTRUMENTATION

The basic idea of WAIL is to send a short-pulse, narrow-beam laser into a cloud, and record, as a function of both space and time, the intensity of the returning light over a wide field of view (Davis et al. 1997, 1999). In essence, one wants to take a "movie" of the propagation of the multiply-scattered light. The first realization of such a fully imaging WAIL instrument (Love et al., 2001) relies on unique imaging detector technology developed at Los Alamos National Laboratory, Priedhorsky et al.'s (1996) Micro-channel Plate/Crossed Delay Line (MCP/CDL) detector coupled with high-speed pulse absolute timing electronics. The MCP/CDL technology features photon-counting sensitivity, effectively up to ~1500^2 pixels, and ultra-high time resolution (100 ps). It consists of the MCP/CDL detector — a photo-cathode coated vacuum tube, intensified by micro-channel plates, read out by a crossed delay line anode — together with fast pulse-timing electronics. Each photo-electron is intensified by a factor of 10^7, with positional information preserved, by the MCP. The electron cloud is collected by helically wound delay lines, producing in each line two counter-propagating current pulses which emerge from the ends. By measuring the arrival times of the pulses at the ends of the delay lines, the position of the original photon event is determined; with two orthogonal delay lines, both the *x*- and *y*- coordinates are determined. This unique strategy for extracting spatial information distinguishes the MCP/CDL from other sensitive imagers such as gated/intensified CCDs. As an early test, we exploited the extremely high time resolution (100 ps corresponds to a path-length of only 3 cm) to perform laboratory-scale simulations of off-beam lidar, where the "cloud" was an aquarium filled with a scattering liquid suspension (Davis et al. 1998).

This detector is not only capable of performing at very low light-levels, but actually requires them: too high a count rate (>5×10^6/sec over the entire detector) confuses the timing-based imaging scheme. This count rate limit demands a high laser repetition rate and averaging over many pulses. Repetition rate around 5–15 kHz is ideal, permitting maximal pulse averaging while avoiding the return from one pulse overlapping with the next. The MCP's spectral response makes a 532 nm frequency-doubled Nd:YAG laser a good choice. Our laser produces 0.2–0.5 mJ/pulse at a variable rep rate (12 kHz is typical for us), with pulse widths ranging from 30 ns to 50 ns depending on operating conditions. The laser is triggered by a master clock, which also provides the timing reference for the detector system electronics.

This nighttime WAIL implementation uses a standard medium-format camera lens with a 35 mm focal length to feed the detector, thus obtaining a full-angle FOV of 60°. This wide angle is needed for ground-based measurements, because the high-order scattering tail of interest here extends up to a kilometer from the beam, a distance comparable to the typical range to the cloud base. One challenge in this experiment is the large dynamic range, several orders of magnitude, between the initial return (the traditional on-beam lidar signal) and the multiply scattered returns from locations at very large displacements from the beam. The faint large-displacement returns require a band-pass filter, ≈10 nm wide for nighttime work, to reject as much background light as possible. The use of interference filters presents an apparent problem, given the wide field of view, since, as is well known, the band center for standard interference filters varies strongly with angle of incidence. Over the 30° half-angle range of our system, the passband center wavelength shifts nearly 15 nm to shorter wavelengths as one moves from the center to the edge of the field. This angular sensitivity, however, can be put to use to partially cancel the strong center-to-edge gradient intrinsic to cloud returns but challenging to any detector system, particularly to our

* *Corresponding author:* Steven P. Love, LANL, MS C323, Los Alamos, NM 87545; 505 667-0067; fax 505 667-3815; email: splove@lanl.gov.

MCP/CDL. If, instead of a filter centered (at normal incidence) at the laser wavelength, one chooses a somewhat longer nominal filter wavelength, light at large angles of incidence (i.e., coming from the edge of the FOV) will be near the angle-shifted center of the filter passband, while light near normal incidence (i.e., coming from the bright central spot) will be in the wings of the filter passband and be strongly attenuated. The resulting images in this case will show a bright annular region of strong transmission with a dark center.

Our second implementation of the WAIL concept, recently deployed in an experiment at the DOE Atmospheric Radiation Measurements (ARM) program Cloud and Radiation Testbed (CART) site in Oklahoma, makes use of a commercial (Roper Scientific/Princeton Instruments "PI-Max") intensified gated CCD as the receiver. For this 18 mm detector array, we use a lens with 12.5 mm focal-length, resulting in a 70° square field of view. To keep data volumes manageable, we bin the original 512x512 pixel images down to 128x128 pixels.

The gated/intensified CCD detector technology, like the MCP/CDL, uses a micro-channel plate photomultiplier, but there the similarity ends. First, the MCP/CDL has an ultimate time resolution of 100 ps, compared to 2 ns for the CCD system, but this difference is unimportant for cloud measurements where relevant time scales are tens of ns and longer. More important are the differences in the basic modes of operation. Unlike the MCP/CDL system, which time-tags each photon as it arrives, producing raw data consisting of a long stream of time- and space-tagged photon events, the gated CCD system achieves time resolution by electronically gating the intensifier, with gate delay and gate width as adjustable parameters. The MCP/CDL system collects an entire time series for each laser pulse (although only a few photons per pulse can be collected), with good statistics achieved by integrating results for many pulses. The intensified gated CCD, in contrast, collects returns for a single delay time (determined by the gate delay setting), again integrating multiple pulses to achieve good statistics, then advances the gate delay relative to the laser trigger to collect the next "movie frame." There are advantages and disadvantages to both approaches. The CCD can collect many more photons per laser pulse than the MCP/CDL system, the latter being severely constrained by its pulse-timing imaging scheme. Also, the programmable, adjustable gate width of the CCD system allows the exposure time to be adjusted automatically during the course of the measurement, with short exposures for the bright early returns, and longer exposures for the dim high-order scattering. This considerably ameliorates the problems caused by the large dynamic range of the cloud-scattered returns. On the other hand, both systems require total integration times on the order of a minute to collect a complete scattering "movie" with good statistics, and clouds can change on this time scale. The MCP/CDL has the advantage of collecting complete time sequences for each shot, with the result that a time-varying cloud is simply averaged in a straightforward manner in the final multi-pulse integrated data set. But if the cloud changes significantly during measurement with the CCD system, the beginning and end of the time sequence may correspond to very different clouds. Thus with a rapidly varying cloud deck, it is necessary to average many CCD data sets to achieve well-averaged data comparable to that obtained with the MCP/CDL version.

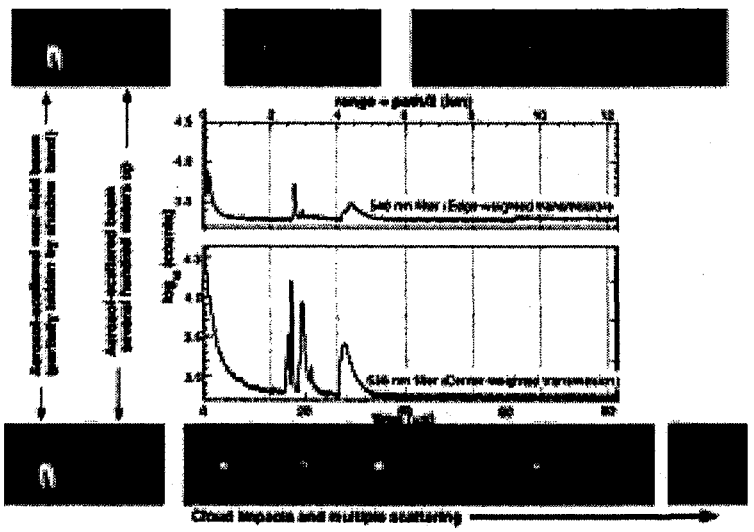

Figure 1: *Nighttime WAIL results using the MCP/CDL detector system.* Shown here are the spatially integrated total return as a function of time (graphs) and a sequence of selected frames from the corresponding WAIL "movies" which show the spatial distribution of the returning light as a function of time. The full-angle FOV is approximately 60°. Two data sets for essentially the same cloud deck are shown, being taken a just few minutes apart. These were obtained with two different filters on the optics, one that emphasizes the large-angle returns (top) and the other emphasizing the center region (bottom). Narrow bandpass interference filters are generally used to reject background light, but also affect the spatial response of the system (see text). Each sequence begins with the Rayleigh/aerosol-scattered beam as it leaves the laser (located off the bottom right side of the FOV); a shadowband blocks the brightest portion of this early return. For these early times, the system is effectively bistatic. Subsequent frames show the aerosol-scattered pulse several hundred meters up, the initial impact on the cloud deck, and subsequent spreading due to multiple scattering. Notice the multiple layers in the lower (smaller-angle) plot.

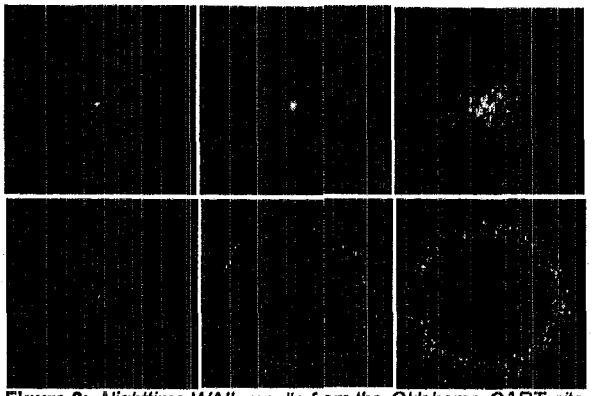

Figure 2: *Nighttime WAIL results from the Oklahoma CART site,* March 24, 2002, using the gated intensified CCD detector system. Top row shows representative WAIL time slices, showing cloud impact and subsequent spreading, using the 536 nm band center interference filter, which passes the center region while suppressing the large angle scattering. Bottom row shows corresponding frames from a data set using the 546 nm filter, which passes returns from the edge of the FOV. Field of view of each frame is 70 degrees. CCD gate width is 50 ns.

Figures 1 and 2 show representative results from the two detector systems Figure 1 shows nighttime results for a multi-layer cloud deck, probed with two different filters on the MCP/CDL detector, one (nominal band center at 540 nm) which strongly suppresses the center spot, and the other (nominal band center at 536 nm) providing a more uniform response across the field. In each case, the spatially integrated return as a function of time (i.e. the temporal Green function) is plotted, along with representative frames of the spatial WAIL "movie," each frame showing the full 60° FOV. Figure 2 shows sample frames from CCD data sets collected at DOE's Southern Great Plains Cloud and Radiation Testbed (CART) site, again with two interference filters, this time 536 nm and 546 nm.

In both cases, we see cloud-base impacts followed by a strong spreading due to multiple scattering in the highest/densest layer. For QuickTime™ movie versions of these and other datasets, see http://nis-www.lanl.gov/~love/clouds.html.

3. TOWARDS A DAYTIME-CAPABLE WAIL

We are presently developing daylight capability for WAIL by means of an ultra-narrow magneto-optic filter coincident with strong solar Fraunhofer absorption lines. This filter uses Faraday rotation in sodium vapor to produce a 90° rotation of the plane of polarization for light propagating along the direction of the applied magnetic field. Placed between crossed polarizers, this results in an extremely narrow transmission band centered at the Na lines (Agnelli et al. 1975). Apart from their extreme narrowness and the convenient coincidence with the Na Fraunhofer lines, their most important feature for WAIL is that, unlike interference filters, their bandpass wavelength is nearly independent of the angle of incidence, at least for small angles. This is because the Faraday rotation is proportional to both the dot product of the direction of propagation and the B-field direct (~cosθ), and to the distance traveled through the Na vapor (~ 1/cosθ), the two angular terms thus canceling. We have built a sodium Faraday filter incorporating internal optics to provide a 60° external field of view while keeping the internal range of angles within the Na vapor cell to less than 20°. Shown in Fig. 3 (left hand side), it uses SmCo permanent magnets to produce a 2700 gauss field inside the Na cell. The expected transmission characteristics, calculated using the model of Chen et al. (1993) are also shown in Fig. 3 (right hand side). Detailed verification of this curve is awaiting completion of the dye laser system that will be used as the transmitter in the daylight WAIL system.

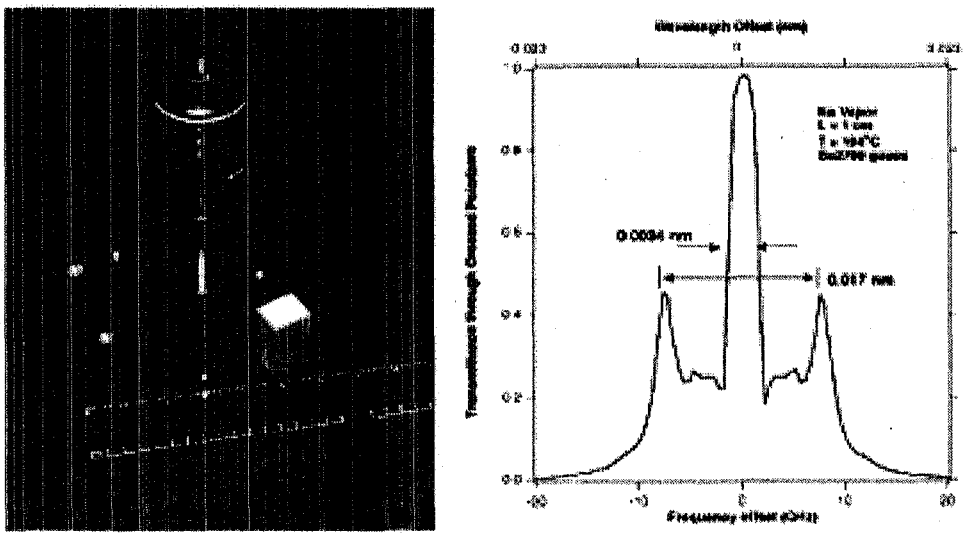

Figure 3: *Wide-angle Na Faraday atomic line filter.* Left: photograph of the assembled filter with one its eight SmCo magnets partially withdrawn. Right: calculated transmittance of the filter; center wavelength is 589 nm.

4. WAIL RETRIEVALS OF CLOUD PROPERTIES

In previous papers (Davis et al. 1997, 1999), we gave detailed theoretical treatments of off-beam lidar in the diffusion regime, both analytical and numerical Monte Carlo modeling. Here we present only a brief summary of the key results relevant to interpreting WAIL data.

At this point in time, we only use two average quantities from the space-time WAIL data: mean in-cloud pathlength $\langle\lambda\rangle$, and root-mean square horizontal displacement $\langle\rho^2\rangle^{1/2}$. In the following, it is only important to know that these two observables have different dependencies on "rescaled" cloud optical depth $(1-g)\tau$ where g is the asymmetry factor of the scattering phase function. Figure 4 shows how the cloud parameters are obtained from the data using the example in Fig. 1.

Apart from merging the datasets from the more- and less off-beam filters in Fig. 1, the only parts of the data analysis that requires human intervention is to manually define cloud-base and the laser impact point in the temporal and spatial domains as well as find the noise-level to subtract.

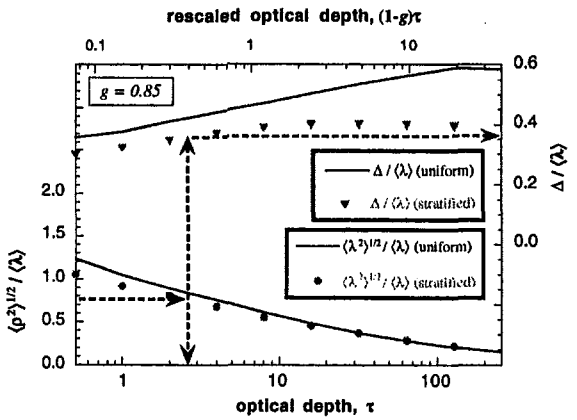

Figure 4: *Retrieval of cloud properties from the data in Fig. 1.* The lower curve shows calculated ratios of two different 2nd-order moments to the 1st-order moment of the pathlength distribution. It is plotted vs. optical depth for a uniform cloud (line) and for a more realistic stratified cloud (symbols) in for ground-based observation. The upper curves are calculated ratios of the cloud thickness to mean pathlength. All computations used an asymmetry factor of $g = 0.85$. Ratio values measured with WAIL (cf. Sect. 2) are indicated by the lower dashed horizontal line, whose intersection with the lower curve gives the optical depth. From there, a vertical line to the upper curve yields the thickness Δ; the mean pathlength was found to be approximately 1.37 km, yielding a physical cloud thickness of 0.52 km.

5. CONCLUSION AND OUTLOOK

Off-beam lidar has advanced rapidly since its inception in the year leading up to Davis et al. (1997). Furthermore, the WAIL project at LANL is not the only one engaged in off-beam lidar development. At NASA-GSFC, Dr. Robert Cahalan has been spearheading the THickness from Off-beam Returns (THOR) project, an airborne design recently deployed for validation at the ARM site (at the same time as WAIL with its new detector), over the same timeframe. Drs. K. F. Evans (U. of Colorado/PAOS) and P. Lawson (Spec, Inc.) are testing an "in-situ" cloud lidar concept based on the same photon diffusion concepts as off-beam lidar. In this case, the aircraft is flying inside the cloud layer rather than far (c. 10 km) above it. As shown by Davis et al. (2001), the Lidar In space Technology Experiment (LITE) on a 1994 shuttle mission was a highly successful, if somewhat inadvertent, off-beam cloud lidar without any spatial resolution, only time; cloud property retrievals are still possible.

We therefore anticipate a bright future for lidar techniques that fully exploit —rather than avoid or mitigate— multiple scattering to probe dense clouds.

REFERENCES

Agnelli, C., A. Cacciani, and M. Fofi, 1975: The magneto-optical filter, *Solar Physics*, **44**, 509-518.

Davis, A., D. M. Winker, A. Marshak, J. D. Spinhirne, R. F. Cahalan, S. P. Love, S. H. Melfi, and W. J. Wiscombe, 1997: Retrieval of physical and optical cloud thicknesses from space-borne and wide-angle lidar, n *Advances in Atmospheric Remote Sensing with Lidar*, Eds. A. Ansmann, R. Neuber, P. Rairoux, and U. Wadinger, Springer-Verlag, pp. 193–196.

Chen, H., C. Y. She, P. Searcy, and E. Korevaar, 1993: Sodium-vapor dispersive Faraday filter, *Opt. Lett.*, **18**, 1019-1021.

Davis, A., D. M. Winker, A. Marshak, J. D. Spinhirne, R. F. Cahalan, S. P. Love, S. H. Melfi, and W. J. Wiscombe, 1997: Retrieval of physical and optical cloud thicknesses from space-borne and wide-angle lidar, in *Advances in Atmospheric Remote Sensing with Lidar*. Eds. A. Ansmann, R, Neuber, P. Rairoux, and U. Wadinger, Springer-Verlag, pp. 193-196.

Davis, A. B., R. F. Cahalan, J. D. Spinhirne, M. J. McGill, and S. P. Love, 1999 : Off-beam lidar: An emerging technique in cloud remote sensing based on radiative Green-function theory in the diffusion domain, *Phys. Chem. Earth (B)*, **24**, 757–765.

Davis, A. B., C. Ho, and S. P. Love, 1998: Off-Beam (Multiply-Scattered) Lidar Returns from Stratus, 2: Space-Time Measurements in a Laboratory Simulation, in *19th International Laser Radar Conference Proceedings*, Eds. U. Singh, S. Ismail, and G. Schwemmer, July 6–10, 1998, Annapolis (Md), NASA Center for Aero-Space Information (CASI), pp. 55–58.

Davis, A. B., D. M. Winker, and M. A. Vaughan, 2001: First Retrieval of Boundary-Layer Cloud Properties from Off-Beam/Multiple-Scattering Lidar Data Collected in Space, in *Laser Remote Sensing of the Atmosphere*. Eds. A. Dabas and J. Pelon, École Polytechnique, Palaiseau (France), pp. 35-38.

Love, S. P., A. B. Davis, C. Ho, and C. A. Rohde, 2001: Remote sensing of cloud thickness and liquid water content with Wide-Angle Imaging Lidar," *Atmospheric Research* **59-60**, 295-312.

Priedhorsky, W. C., R. C. Smith, and C. Ho, 1996: Laser ranging and mapping with a photon-counting detector," *Appl. Opt.*, **35**, 441–452.

J5.3 ACTIVE PROBING OF CLOUD THICKNESS AND OPTICAL DEPTH USING WIDE-ANGLE IMAGING LIDAR

Steven P. Love,* Anthony B. Davis, Charles A. Rohde, Larry Tellier, Cheng Ho
Space and Remote Sensing Sciences Group (NIS-2), Los Alamos National Laboratory

1. INTRODUCTION AND OVERVIEW

At most optical wavelengths, laser light in a cloud lidar experiment is not absorbed but merely scattered out of the beam, eventually escaping the cloud via multiple scattering. There is much information available in this light scattered far from the input beam, information ignored by traditional "on-beam" lidar. Monitoring these off-beam returns in a fully space- and time-resolved manner is the essence of our unique instrument, Wide Angle Imaging Lidar (WAIL). In effect, WAIL produces wide-field (60° full-angle) "movies" of the scattering process and records the cloud's radiative Green functions. A direct data product of WAIL is the distribution of photon path lengths resulting from multiple scattering in the cloud. Following insights from diffusion theory, we can use the measured Green functions to infer the physical thickness and optical depth of the cloud layer. WAIL is notable in that it is applicable to optically thick clouds, a regime in which traditional lidar is reduced to ceilometry.

Section 2 covers the up-to-date evolution of the nighttime WAIL instrument at LANL. Section 3 reports our progress towards daytime capability for WAIL, an important extension to full diurnal cycle monitoring by means of an ultra-narrow magneto-optic atomic line filter. Section 4 describes briefly how the important cloud properties can be inferred from WAIL signals.

2. EVOLUTION OF WAIL INSTRUMENTATION

The basic idea of WAIL is to send a short-pulse, narrow-beam laser into a cloud, and record, as a function of both space and time, the intensity of the returning light over a wide field of view (Davis et al. 1997, 1999). In essence, one wants to take a "movie" of the propagation of the multiply-scattered light. The first realization of such a fully imaging WAIL instrument (Love et al., 2001) relies on unique imaging detector technology developed at Los Alamos National Laboratory, Priedhorsky et al.'s (1996) Micro-channel Plate/Crossed Delay Line (MCP/CDL) detector coupled with high-speed pulse absolute timing electronics. The MCP/CDL technology features photon-counting sensitivity, effectively up to ~1500^2 pixels, and ultra-high time resolution (100 ps). It consists of the MCP/CDL detector — a photo-cathode coated vacuum tube, intensified by micro-channel plates, read out by a crossed delay line anode — together with fast pulse-timing electronics. Each photo-electron is intensified by a factor of 10^7, with positional information preserved, by the MCP. The electron cloud is collected by helically wound delay lines, producing in each line two counter-propagating current pulses which emerge from the ends. By measuring the arrival times of the pulses at the ends of the delay lines, the position of the original photon event is determined; with two orthogonal delay lines, both the x- and y- coordinates are determined. This unique strategy for extracting spatial information distinguishes the MCP/CDL from other sensitive imagers such as gated/intensified CCDs. As an early test, we exploited the extremely high time resolution (100 ps corresponds to a path-length of only 3 cm) to perform laboratory-scale simulations of off-beam lidar, where the "cloud" was an aquarium filled with a scattering liquid suspension (Davis et al. 1998).

This detector is not only capable of performing at very low light-levels, but actually requires them: too high a count rate (>5×10^6/sec over the entire detector) confuses the timing-based imaging scheme. This count rate limit demands a high laser repetition rate and averaging over many pulses. Repetition rate around 5–15 kHz is ideal, permitting maximal pulse averaging while avoiding the return from one pulse overlapping with the next. The MCP's spectral response makes a 532 nm frequency-doubled Nd:YAG laser a good choice. Our laser produces 0.2–0.5 mJ/pulse at a variable rep rate (12 kHz is typical for us), with pulse widths ranging from 30 ns to 50 ns depending on operating conditions. The laser is triggered by a master clock, which also provides the timing reference for the detector system electronics.

This nighttime WAIL implementation uses a standard medium-format camera lens with a 35 mm focal length to feed the detector, thus obtaining a full-angle FOV of 60°. This wide angle is needed for ground-based measurements, because the high-order scattering tail of interest here extends up to a kilometer from the beam, a distance comparable to the typical range to the cloud base. One challenge in this experiment is the large dynamic range, several orders of magnitude, between the initial return (the traditional on-beam lidar signal) and the multiply scattered returns from locations at very large displacements from the beam. The faint large-displacement returns require a band-pass filter, ≈10 nm wide for nighttime work, to reject as much background light as possible. The use of interference filters presents an apparent problem, given the wide field of view, since, as is well known, the band center for standard interference filters varies strongly with angle of incidence. Over the 30° half-angle range of our system, the passband center wavelength shifts nearly 15 nm to shorter wavelengths as one moves from the center to the edge of the field. This angular sensitivity, however, can be put to use to partially cancel the strong center-to-edge gradient intrinsic to cloud returns but challenging to any detector system, particularly to our

* *Corresponding author:* Steven P. Love, LANL, MS C323, Los Alamos, NM 87545; 505 667-0067; fax 505 667-3815; email: splove@lanl.gov.

MCP/CDL. If, instead of a filter centered (at normal incidence) at the laser wavelength, one chooses a somewhat longer nominal filter wavelength, light at large angles of incidence (i.e., coming from the edge of the FOV) will be near the angle-shifted center of the filter passband, while light near normal incidence (i.e., coming from the bright central spot) will be in the wings of the filter passband and be strongly attenuated. The resulting images in this case will show a bright annular region of strong transmission with a dark center.

Our second implementation of the WAIL concept, recently deployed in an experiment at the DOE Atmospheric Radiation Measurements (ARM) program Cloud and Radiation Testbed (CART) site in Oklahoma, makes use of a commercial (Roper Scientific/Princeton Instruments "PI-Max") intensified gated CCD as the receiver. For this 18 mm detector array, we use a lens with 12.5 mm focal-length, resulting in a 70° square field of view. To keep data volumes manageable, we bin the original 512x512 pixel images down to 128x128 pixels.

The gated/intensified CCD detector technology, like the MCP/CDL, uses a micro-channel plate photomultiplier, but there the similarity ends. First, the MCP/CDL has an ultimate time resolution of 100 ps, compared to 2 ns for the CCD system, but this difference is unimportant for cloud measurements where relevant time scales are tens of ns and longer. More important are the differences in the basic modes of operation. Unlike the MCP/CDL system, which time-tags each photon as it arrives, producing raw data consisting of a long stream of time- and space-tagged photon events, the gated CCD system achieves time resolution by electronically gating the intensifier, with gate delay and gate width as adjustable parameters. The MCP/CDL system collects an entire time series for each laser pulse (although only a few photons per pulse can be collected), with good statistics achieved by integrating results for many pulses. The intensified gated CCD, in contrast, collects returns for a single delay time (determined by the gate delay setting), again integrating multiple pulses to achieve good statistics, then advances the gate delay relative to the laser trigger to collect the next "movie frame." There are advantages and disadvantages to both approaches. The CCD can collect many more photons per laser pulse than the MCP/CDL system, the latter being severely constrained by its pulse-timing imaging scheme. Also, the programmable, adjustable gate width of the CCD system allows the exposure time to be adjusted automatically during the course of the measurement, with short exposures for the bright early returns, and longer exposures for the dim high-order scattering. This considerably ameliorates the problems caused by the large dynamic range of the cloud-scattered returns. On the other hand, both systems require total integration times on the order of a minute to collect a complete scattering "movie" with good statistics, and clouds can change on this time scale. The MCP/CDL has the advantage of collecting complete time sequences for each shot, with the result that a time-varying cloud is simply averaged in a straightforward manner in the final multi-pulse integrated data set. But if the cloud changes significantly during measurement with the CCD system, the beginning and end of the time sequence may correspond to very different clouds. Thus with a rapidly varying cloud deck, it is necessary to average many CCD data sets to achieve well-averaged data comparable to that obtained with the MCP/CDL version.

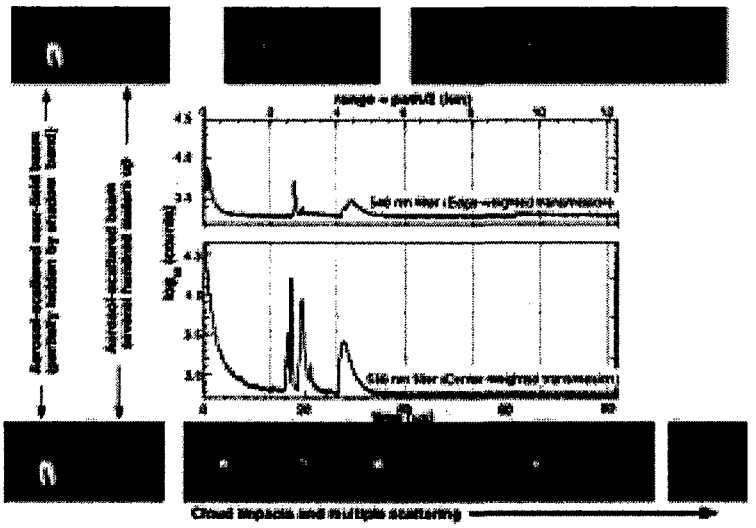

Figure 1: *Nighttime WAIL results using the MCP/CDL detector system.* Shown here are the spatially integrated total return as a function of time (graphs) and a sequence of selected frames from the corresponding WAIL "movies" which show the spatial distribution of the returning light as a function of time. The full-angle FOV is approximately 60°. Two data sets for essentially the same cloud deck are shown, being taken a just few minutes apart. These were obtained with two different filters on the optics, one that emphasizes the large-angle returns (top) and the other emphasizing the center region (bottom). Narrow bandpass interference filters are generally used to reject background light, but also affect the spatial response of the system (see text). Each sequence begins with the Rayleigh/aerosol-scattered beam as it leaves the laser (located off the bottom right side of the FOV); a shadowband blocks the brightest portion of this early return. For these early times, the system is effectively bistatic. Subsequent frames show the aerosol-scattered pulse several hundred meters up, the initial impact on the cloud deck, and subsequent spreading due to multiple scattering. Notice the multiple layers in the lower (smaller-angle) plot.

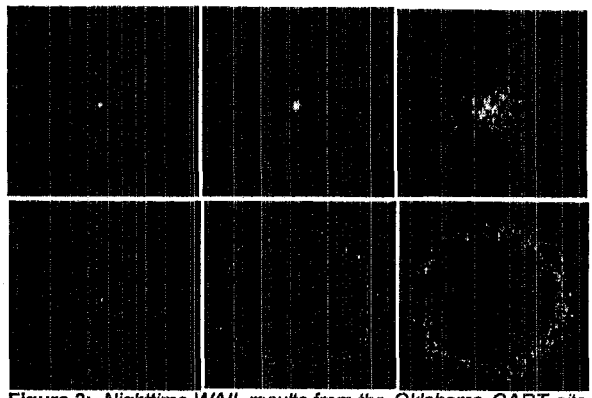

Figure 2: *Nighttime WAIL results from the Oklahoma CART site,* March 24, 2002, using the gated intensified CCD detector system. Top row shows representative WAIL time slices, showing cloud impact and subsequent spreading, using the 536 nm band center interference filter, which passes the center region while suppressing the large angle scattering. Bottom row shows corresponding frames from a data set using the 546 nm filter, which passes returns from the edge of the FOV. Field of view of each frame is 70 degrees. CCD gate width is 50 ns.

Figures 1 and 2 show representative results from the two detector systems Figure 1 shows nighttime results for a multi-layer cloud deck, probed with two different filters on the MCP/CDL detector, one (nominal band center at 540 nm) which strongly suppresses the center spot, and the other (nominal band center at 536 nm) providing a more uniform response across the field. In each case, the spatially integrated return as a function of time (i.e. the temporal Green function) is plotted, along with representative frames of the spatial WAIL "movie," each frame showing the full 60° FOV. Figure 2 shows sample frames from CCD data sets collected at DOE's Southern Great Plains Cloud and Radiation Testbed (CART) site, again with two interference filters, this time 536 nm and 546 nm.

In both cases, we see cloud-base impacts followed by a strong spreading due to multiple scattering in the highest/densest layer. For QuickTime™ movie versions of these and other datasets, see http://nis-www.lanl.gov/~love/clouds.html.

3. TOWARDS A DAYTIME-CAPABLE WAIL

We are presently developing daylight capability for WAIL by means of an ultra-narrow magneto-optic filter coincident with strong solar Fraunhofer absorption lines. This filter uses Faraday rotation in sodium vapor to produce a 90° rotation of the plane of polarization for light propagating along the direction of the applied magnetic field. Placed between crossed polarizers, this results in an extremely narrow transmission band centered at the Na lines (Agnelli et al. 1975). Apart from their extreme narrowness and the convenient coincidence with the Na Fraunhofer lines, their most important feature for WAIL is that, unlike interference filters, their bandpass wavelength is nearly independent of the angle of incidence, at least for small angles. This is because the Faraday rotation is proportional to both the dot product of the direction of propagation and the B-field direct (~cosθ), and to the distance traveled through the Na vapor (~ 1/cosθ), the two angular terms thus canceling. We have built a sodium Faraday filter incorporating internal optics to provide a 60° external field of view while keeping the internal range of angles within the Na vapor cell to less than 20°. Shown in Fig. 3 (left hand side), it uses SmCo permanent magnets to produce a 2700 gauss field inside the Na cell. The expected transmission characteristics, calculated using the model of Chen et al. (1993) are also shown in Fig. 3 (right hand side). Detailed verification of this curve is awaiting completion of the dye laser system that will be used as the transmitter in the daylight WAIL system.

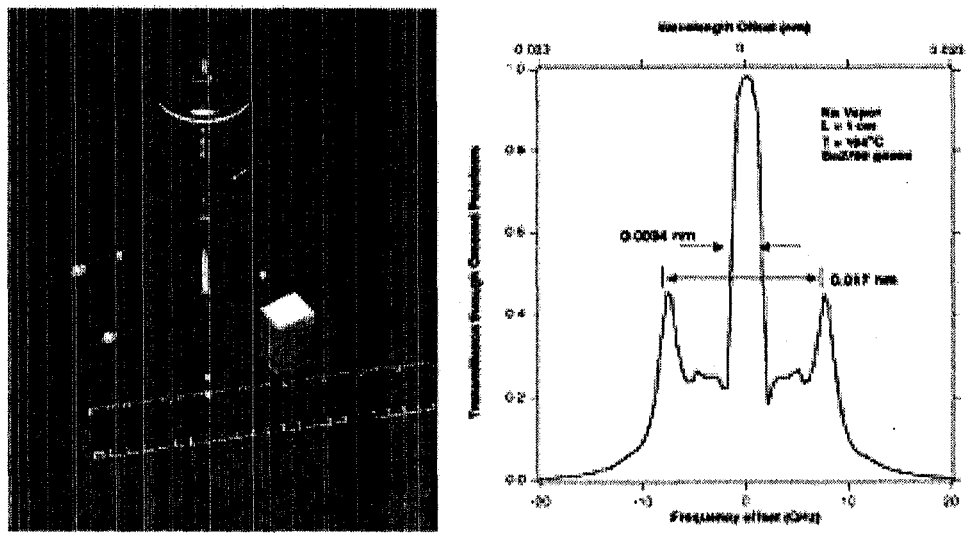

Figure 3: *Wide-angle Na Faraday atomic line filter.* Left: photograph of the assembled filter with one its eight SmCo magnets partially withdrawn. Right: calculated transmittance of the filter; center wavelength is 589 nm.

4. WAIL RETRIEVALS OF CLOUD PROPERTIES

In previous papers (Davis et al. 1997, 1999), we gave detailed theoretical treatments of off-beam lidar in the diffusion regime, both analytical and numerical Monte Carlo modeling. Here we present only a brief summary of the key results relevant to interpreting WAIL data.

At this point in time, we only use two average quantities from the space-time WAIL data: mean in-cloud pathlength $\langle\lambda\rangle$, and root-mean square horizontal displacement $\langle\rho^2\rangle^{1/2}$. In the following, it is only important to know that these two observables have different dependencies on "rescaled" cloud optical depth $(1-g)\tau$ where g is the asymmetry factor of the scattering phase function. Figure 4 shows how the cloud parameters are obtained from the data using the example in Fig. 1.

Apart from merging the datasets from the more- and less off-beam filters in Fig. 1, the only parts of the data analysis that requires human intervention is to manually define cloud-base and the laser impact point in the temporal and spatial domains as well as find the noise-level to subtract.

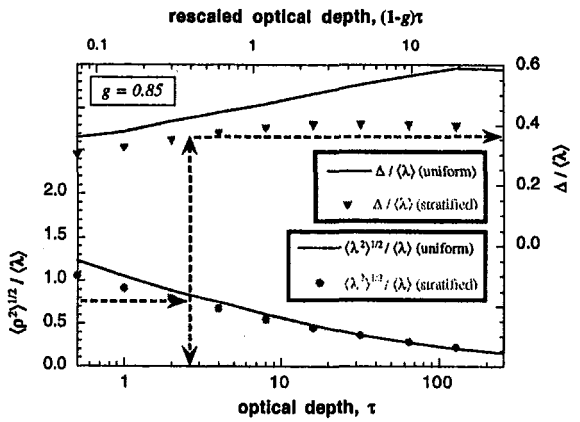

Figure 4: *Retrieval of cloud properties from the data in Fig. 1.* The lower curve shows calculated ratios of two different 2nd-order moments to the 1st-order moment of the pathlength distribution. It is plotted vs. optical depth for a uniform cloud (line) and for a more realistic stratified cloud (symbols) in for ground-based observation. The upper curves are calculated ratios of the cloud thickness to mean pathlength. All computations used an asymmetry factor of $g = 0.85$. Ratio values measured with WAIL (cf. Sect. 2) are indicated by the lower dashed horizontal line, whose intersection with the lower curve gives the optical depth. From there, a vertical line to the upper curve yields the thickness Δ; the mean pathlength was found to be approximately 1.37 km, yielding a physical cloud thickness of 0.52 km.

5. CONCLUSION AND OUTLOOK

Off-beam lidar has advanced rapidly since its inception in the year leading up to Davis et al. (1997). Furthermore, the WAIL project at LANL is not the only one engaged in off-beam lidar development. At NASA-GSFC, Dr. Robert Cahalan has been spearheading the THickness from Off-beam Returns (THOR) project, an airborne design recently deployed for validation at the ARM site (at the same time as WAIL with its new detector), over the same timeframe. Drs. K. F. Evans (U. of Colorado/PAOS) and P. Lawson (Spec, Inc.) are testing an "in-situ" cloud lidar concept based on the same photon diffusion concepts as off-beam lidar. In this case, the aircraft is flying inside the cloud layer rather than far (c. 10 km) above it. As shown by Davis et al. (2001), the Lidar In space Technology Experiment (LITE) on a 1994 shuttle mission was a highly successful, if somewhat inadvertent, off-beam cloud lidar without any spatial resolution, only time; cloud property retrievals are still possible.

We therefore anticipate a bright future for lidar techniques that fully exploit —rather than avoid or mitigate— multiple scattering to probe dense clouds.

REFERENCES

Agnelli, C., A. Cacciani, and M. Fofi, 1975: The magneto-optical filter, *Solar Physics*, **44**, 509-518.

Davis, A., D. M. Winker, A. Marshak, J. D. Spinhirne, R. F. Cahalan, S. P. Love, S. H. Melfi, and W. J. Wiscombe, 1997: Retrieval of physical and optical cloud thicknesses from space-borne and wide-angle lidar, n *Advances in Atmospheric Remote Sensing with Lidar*, Eds. A. Ansmann, R. Neuber, P. Rairoux, and U. Wadinger, Springer-Verlag, pp. 193–196.

Chen, H., C. Y. She, P. Searcy, and E. Korevaar, 1993: Sodium-vapor dispersive Faraday filter, *Opt. Lett.*, **18**, 1019-1021.

Davis, A., D. M. Winker, A. Marshak, J. D. Spinhirne, R. F. Cahalan, S. P. Love, S. H. Melfi, and W. J. Wiscombe, 1997: Retrieval of physical and optical cloud thicknesses from space-borne and wide-angle lidar, in *Advances in Atmospheric Remote Sensing with Lidar*. Eds. A. Ansmann, R, Neuber, P. Rairoux, and U. Wadinger, Springer-Verlag, pp. 193-196.

Davis, A. B., R. F. Cahalan, J. D. Spinhirne, M. J. McGill, and S. P. Love, 1999 : Off-beam lidar: An emerging technique in cloud remote sensing based on radiative Green-function theory in the diffusion domain, *Phys. Chem. Earth (B)*, **24**, 757–765.

Davis, A. B., C. Ho, and S. P. Love, 1998: Off-Beam (Multiply-Scattered) Lidar Returns from Stratus, 2: Space-Time Measurements in a Laboratory Simulation, in *19th International Laser Radar Conference Proceedings*, Eds. U. Singh, S. Ismail, and G. Schwemmer, July 6–10, 1998, Annapolis (Md), NASA Center for Aero-Space Information (CASI), pp. 55–58.

Davis, A. B., D. M. Winker, and M. A. Vaughan, 2001: First Retrieval of Boundary-Layer Cloud Properties from Off-Beam/Multiple-Scattering Lidar Data Collected in Space, in *Laser Remote Sensing of the Atmosphere*. Eds. A. Dabas and J. Pelon, École Polytechnique, Palaiseau (France), pp. 35-38.

Love, S. P., A. B. Davis, C. Ho, and C. A. Rohde, 2001: Remote sensing of cloud thickness and liquid water content with Wide-Angle Imaging Lidar," *Atmospheric Research* **59-60**, 295-312.

Priedhorsky, W. C., R. C. Smith, and C. Ho, 1996: Laser ranging and mapping with a photon-counting detector," *Appl. Opt.*, **35**, 441–452.

J5.3 ACTIVE PROBING OF CLOUD THICKNESS AND OPTICAL DEPTH USING WIDE-ANGLE IMAGING LIDAR

Steven P. Love,* Anthony B. Davis, Charles A. Rohde, Larry Tellier, Cheng Ho
Space and Remote Sensing Sciences Group (NIS-2), Los Alamos National Laboratory

1. INTRODUCTION AND OVERVIEW

At most optical wavelengths, laser light in a cloud lidar experiment is not absorbed but merely scattered out of the beam, eventually escaping the cloud via multiple scattering. There is much information available in this light scattered far from the input beam, information ignored by traditional "on-beam" lidar. Monitoring these off-beam returns in a fully space- and time-resolved manner is the essence of our unique instrument, Wide Angle Imaging Lidar (WAIL). In effect, WAIL produces wide-field (60° full-angle) "movies" of the scattering process and records the cloud's radiative Green functions. A direct data product of WAIL is the distribution of photon path lengths resulting from multiple scattering in the cloud. Following insights from diffusion theory, we can use the measured Green functions to infer the physical thickness and optical depth of the cloud layer. WAIL is notable in that it is applicable to optically thick clouds, a regime in which traditional lidar is reduced to ceilometry.

Section 2 covers the up-to-date evolution of the nighttime WAIL instrument at LANL. Section 3 reports our progress towards daytime capability for WAIL, an important extension to full diurnal cycle monitoring by means of an ultra-narrow magneto-optic atomic line filter. Section 4 describes briefly how the important cloud properties can be inferred from WAIL signals.

2. EVOLUTION OF WAIL INSTRUMENTATION

The basic idea of WAIL is to send a short-pulse, narrow-beam laser into a cloud, and record, as a function of both space and time, the intensity of the returning light over a wide field of view (Davis et al. 1997, 1999). In essence, one wants to take a "movie" of the propagation of the multiply-scattered light. The first realization of such a fully imaging WAIL instrument (Love et al., 2001) relies on unique imaging detector technology developed at Los Alamos National Laboratory, Priedhorsky et al.'s (1996) Micro-channel Plate/Crossed Delay Line (MCP/CDL) detector coupled with high-speed pulse absolute timing electronics. The MCP/CDL technology features photon-counting sensitivity, effectively up to ~1500^2 pixels, and ultra-high time resolution (100 ps). It consists of the MCP/CDL detector — a photo-cathode coated vacuum tube, intensified by micro-channel plates, read out by a crossed delay line anode — together with fast pulse-timing electronics. Each photo-electron is intensified by a factor of 10^7, with positional information preserved, by the MCP. The electron cloud is collected by helically wound delay lines, producing in each line two counter-propagating current pulses which emerge from the ends. By measuring the arrival times of the pulses at the ends of the delay lines, the position of the original photon event is determined; with two orthogonal delay lines, both the *x*- and *y*- coordinates are determined. This unique strategy for extracting spatial information distinguishes the MCP/CDL from other sensitive imagers such as gated/intensified CCDs. As an early test, we exploited the extremely high time resolution (100 ps corresponds to a path-length of only 3 cm) to perform laboratory-scale simulations of off-beam lidar, where the "cloud" was an aquarium filled with a scattering liquid suspension (Davis et al. 1998).

This detector is not only capable of performing at very low light-levels, but actually requires them: too high a count rate (>5×10^6/sec over the entire detector) confuses the timing-based imaging scheme. This count rate limit demands a high laser repetition rate and averaging over many pulses. Repetition rate around 5–15 kHz is ideal, permitting maximal pulse averaging while avoiding the return from one pulse overlapping with the next. The MCP's spectral response makes a 532 nm frequency-doubled Nd:YAG laser a good choice. Our laser produces 0.2–0.5 mJ/pulse at a variable rep rate (12 kHz is typical for us), with pulse widths ranging from 30 ns to 50 ns depending on operating conditions. The laser is triggered by a master clock, which also provides the timing reference for the detector system electronics.

This nighttime WAIL implementation uses a standard medium-format camera lens with a 35 mm focal length to feed the detector, thus obtaining a full-angle FOV of 60°. This wide angle is needed for ground-based measurements, because the high-order scattering tail of interest here extends up to a kilometer from the beam, a distance comparable to the typical range to the cloud base. One challenge in this experiment is the large dynamic range, several orders of magnitude, between the initial return (the traditional on-beam lidar signal) and the multiply scattered returns from locations at very large displacements from the beam. The faint large-displacement returns require a band-pass filter, ≈10 nm wide for nighttime work, to reject as much background light as possible. The use of interference filters presents an apparent problem, given the wide field of view, since, as is well known, the band center for standard interference filters varies strongly with angle of incidence. Over the 30° half-angle range of our system, the passband center wavelength shifts nearly 15 nm to shorter wavelengths as one moves from the center to the edge of the field. This angular sensitivity, however, can be put to use to partially cancel the strong center-to-edge gradient intrinsic to cloud returns but challenging to any detector system, particularly to our

* *Corresponding author:* Steven P. Love, LANL, MS C323, Los Alamos, NM 87545; 505 667-0067; fax 505 667-3815; email: splove@lanl.gov.

MCP/CDL. If, instead of a filter centered (at normal incidence) at the laser wavelength, one chooses a somewhat longer nominal filter wavelength, light at large angles of incidence (i.e., coming from the edge of the FOV) will be near the angle-shifted center of the filter passband, while light near normal incidence (i.e., coming from the bright central spot) will be in the wings of the filter passband and be strongly attenuated. The resulting images in this case will show a bright annular region of strong transmission with a dark center.

Our second implementation of the WAIL concept, recently deployed in an experiment at the DOE Atmospheric Radiation Measurements (ARM) program Cloud and Radiation Testbed (CART) site in Oklahoma, makes use of a commercial (Roper Scientific/Princeton Instruments "PI-Max") intensified gated CCD as the receiver. For this 18 mm detector array, we use a lens with 12.5 mm focal-length, resulting in a 70° square field of view. To keep data volumes manageable, we bin the original 512x512 pixel images down to 128x128 pixels.

The gated/intensified CCD detector technology, like the MCP/CDL, uses a micro-channel plate photomultiplier, but there the similarity ends. First, the MCP/CDL has an ultimate time resolution of 100 ps, compared to 2 ns for the CCD system, but this difference is unimportant for cloud measurements where relevant time scales are tens of ns and longer. More important are the differences in the basic modes of operation. Unlike the MCP/CDL system, which time-tags each photon as it arrives, producing raw data consisting of a long stream of time- and space-tagged photon events, the gated CCD system achieves time resolution by electronically gating the intensifier, with gate delay and gate width as adjustable parameters. The MCP/CDL system collects an entire time series for each laser pulse (although only a few photons per pulse can be collected), with good statistics achieved by integrating results for many pulses. The intensified gated CCD, in contrast, collects returns for a single delay time (determined by the gate delay setting), again integrating multiple pulses to achieve good statistics, then advances the gate delay relative to the laser trigger to collect the next "movie frame." There are advantages and disadvantages to both approaches. The CCD can collect many more photons per laser pulse than the MCP/CDL system, the latter being severely constrained by its pulse-timing imaging scheme. Also, the programmable, adjustable gate width of the CCD system allows the exposure time to be adjusted automatically during the course of the measurement, with short exposures for the bright early returns, and longer exposures for the dim high-order scattering. This considerably ameliorates the problems caused by the large dynamic range of the cloud-scattered returns. On the other hand, both systems require total integration times on the order of a minute to collect a complete scattering "movie" with good statistics, and clouds can change on this time scale. The MCP/CDL has the advantage of collecting complete time sequences for each shot, with the result that a time-varying cloud is simply averaged in a straightforward manner in the final multi-pulse integrated data set. But if the cloud changes significantly during measurement with the CCD system, the beginning and end of the time sequence may correspond to very different clouds. Thus with a rapidly varying cloud deck, it is necessary to average many CCD data sets to achieve well-averaged data comparable to that obtained with the MCP/CDL version.

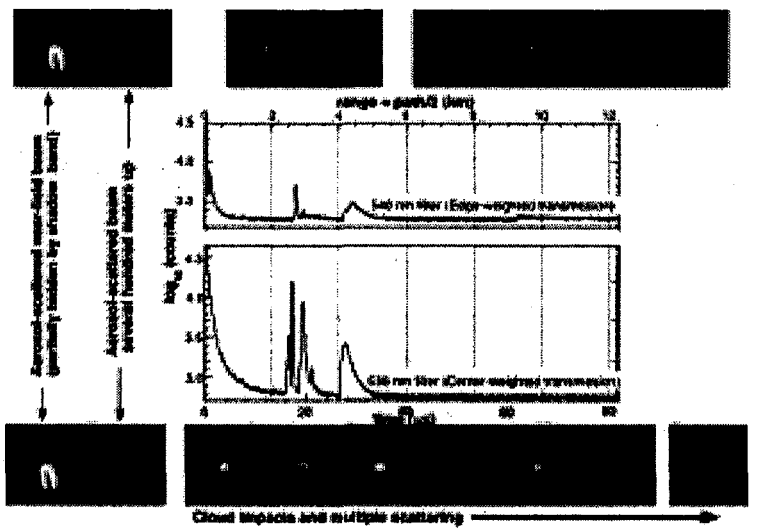

Figure 1: *Nighttime WAIL results using the MCP/CDL detector system.* Shown here are the spatially integrated total return as a function of time (graphs) and a sequence of selected frames from the corresponding WAIL "movies" which show the spatial distribution of the returning light as a function of time. The full-angle FOV is approximately 60°. Two data sets for essentially the same cloud deck are shown, being taken a just few minutes apart. These were obtained with two different filters on the optics, one that emphasizes the large-angle returns (top) and the other emphasizing the center region (bottom). Narrow bandpass interference filters are generally used to reject background light, but also affect the spatial response of the system (see text). Each sequence begins with the Rayleigh/aerosol-scattered beam as it leaves the laser (located off the bottom right side of the FOV); a shadowband blocks the brightest portion of this early return. For these early times, the system is effectively bistatic. Subsequent frames show the aerosol-scattered pulse several hundred meters up, the initial impact on the cloud deck, and subsequent spreading due to multiple scattering. Notice the multiple layers in the lower (smaller-angle) plot.

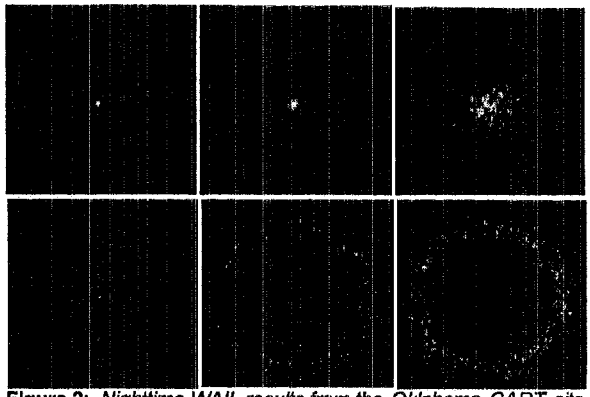

Figure 2: *Nighttime WAIL results from the Oklahoma CART site,* March 24, 2002, using the gated intensified CCD detector system. Top row shows representative WAIL time slices, showing cloud impact and subsequent spreading, using the 536 nm band center interference filter, which passes the center region while suppressing the large angle scattering. Bottom row shows corresponding frames from a data set using the 546 nm filter, which passes returns from the edge of the FOV. Field of view of each frame is 70 degrees. CCD gate width is 50 ns.

Figures 1 and 2 show representative results from the two detector systems Figure 1 shows nighttime results for a multi-layer cloud deck, probed with two different filters on the MCP/CDL detector, one (nominal band center at 540 nm) which strongly suppresses the center spot, and the other (nominal band center at 536 nm) providing a more uniform response across the field. In each case, the spatially integrated return as a function of time (i.e. the temporal Green function) is plotted, along with representative frames of the spatial WAIL "movie," each frame showing the full 60° FOV. Figure 2 shows sample frames from CCD data sets collected at DOE's Southern Great Plains Cloud and Radiation Testbed (CART) site, again with two interference filters, this time 536 nm and 546 nm.

In both cases, we see cloud-base impacts followed by a strong spreading due to multiple scattering in the highest/densest layer. For QuickTime™ movie versions of these and other datasets, see http://nis-www.lanl.gov/~love/clouds.html.

3. TOWARDS A DAYTIME-CAPABLE WAIL

We are presently developing daylight capability for WAIL by means of an ultra-narrow magneto-optic filter coincident with strong solar Fraunhofer absorption lines. This filter uses Faraday rotation in sodium vapor to produce a 90° rotation of the plane of polarization for light propagating along the direction of the applied magnetic field. Placed between crossed polarizers, this results in an extremely narrow transmission band centered at the Na lines (Agnelli et al. 1975). Apart from their extreme narrowness and the convenient coincidence with the Na Fraunhofer lines, their most important feature for WAIL is that, unlike interference filters, their bandpass wavelength is nearly independent of the angle of incidence, at least for small angles. This is because the Faraday rotation is proportional to both the dot product of the direction of propagation and the B-field direct (~cosθ), and to the distance traveled through the Na vapor (~ 1/cosθ), the two angular terms thus canceling. We have built a sodium Faraday filter incorporating internal optics to provide a 60° external field of view while keeping the internal range of angles within the Na vapor cell to less than 20°. Shown in Fig. 3 (left hand side), it uses SmCo permanent magnets to produce a 2700 gauss field inside the Na cell. The expected transmission characteristics, calculated using the model of Chen et al. (1993) are also shown in Fig. 3 (right hand side). Detailed verification of this curve is awaiting completion of the dye laser system that will be used as the transmitter in the daylight WAIL system.

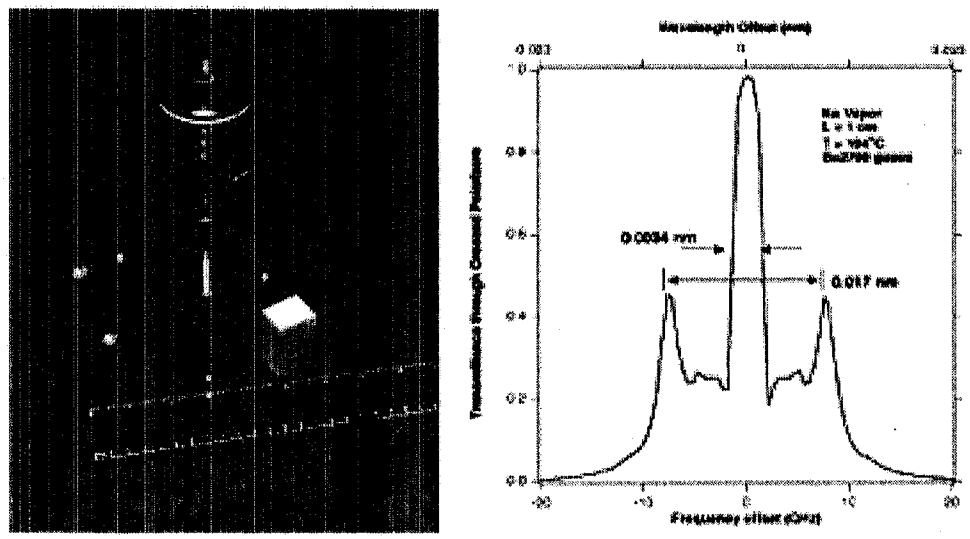

Figure 3: *Wide-angle Na Faraday atomic line filter.* Left: photograph of the assembled filter with one its eight SmCo magnets partially withdrawn. Right: calculated transmittance of the filter; center wavelength is 589 nm.

4. WAIL RETRIEVALS OF CLOUD PROPERTIES

In previous papers (Davis et al. 1997, 1999), we gave detailed theoretical treatments of off-beam lidar in the diffusion regime, both analytical and numerical Monte Carlo modeling. Here we present only a brief summary of the key results relevant to interpreting WAIL data.

At this point in time, we only use two average quantities from the space-time WAIL data: mean in-cloud pathlength $\langle\lambda\rangle$, and root-mean square horizontal displacement $\langle\rho^2\rangle^{1/2}$. In the following, it is only important to know that these two observables have different dependencies on "rescaled" cloud optical depth $(1-g)\tau$ where g is the asymmetry factor of the scattering phase function. Figure 4 shows how the cloud parameters are obtained from the data using the example in Fig. 1.

Apart from merging the datasets from the more- and less off-beam filters in Fig. 1, the only parts of the data analysis that requires human intervention is to manually define cloud-base and the laser impact point in the temporal and spatial domains as well as find the noise-level to subtract.

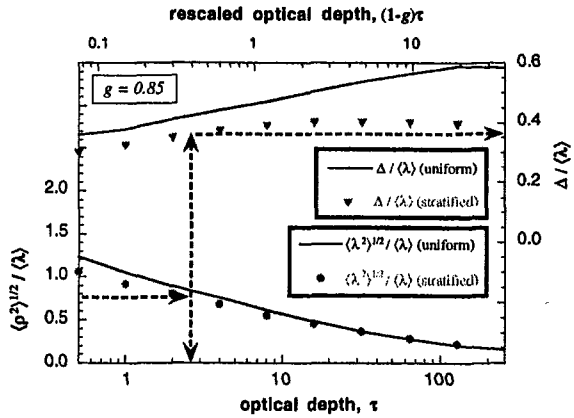

Figure 4: *Retrieval of cloud properties from the data in Fig. 1.* The lower curve shows calculated ratios of two different 2nd-order moments to the 1st-order moment of the pathlength distribution. It is plotted vs. optical depth for a uniform cloud (line) and for a more realistic stratified cloud (symbols) in for ground-based observation. The upper curves are calculated ratios of the cloud thickness to mean pathlength. All computations used an asymmetry factor of $g = 0.85$. Ratio values measured with WAIL (cf. Sect. 2) are indicated by the lower dashed horizontal line, whose intersection with the lower curve gives the optical depth. From there, a vertical line to the upper curve yields the thickness Δ; the mean pathlength was found to be approximately 1.37 km, yielding a physical cloud thickness of 0.52 km.

5. CONCLUSION AND OUTLOOK

Off-beam lidar has advanced rapidly since its inception in the year leading up to Davis et al. (1997). Furthermore, the WAIL project at LANL is not the only one engaged in off-beam lidar development. At NASA-GSFC, Dr. Robert Cahalan has been spearheading the THickness from Off-beam Returns (THOR) project, an airborne design recently deployed for validation at the ARM site (at the same time as WAIL with its new detector), over the same timeframe. Drs. K. F. Evans (U. of Colorado/PAOS) and P. Lawson (Spec, Inc.) are testing an "in-situ" cloud lidar concept based on the same photon diffusion concepts as off-beam lidar. In this case, the aircraft is flying inside the cloud layer rather than far (c. 10 km) above it. As shown by Davis et al. (2001), the Lidar In space Technology Experiment (LITE) on a 1994 shuttle mission was a highly successful, if somewhat inadvertent, off-beam cloud lidar without any spatial resolution, only time; cloud property retrievals are still possible.

We therefore anticipate a bright future for lidar techniques that fully exploit —rather than avoid or mitigate— multiple scattering to probe dense clouds.

REFERENCES

Agnelli, C., A. Cacciani, and M. Fofi, 1975: The magneto-optical filter, *Solar Physics*, **44**, 509-518.

Davis, A., D. M. Winker, A. Marshak, J. D. Spinhirne, R. F. Cahalan, S. P. Love, S. H. Melfi, and W. J. Wiscombe, 1997: Retrieval of physical and optical cloud thicknesses from space-borne and wide-angle lidar, n *Advances in Atmospheric Remote Sensing with Lidar*, Eds. A. Ansmann, R. Neuber, P. Rairoux, and U. Wadinger, Springer-Verlag, pp. 193–196.

Chen, H., C. Y. She, P. Searcy, and E. Korevaar, 1993: Sodium-vapor dispersive Faraday filter, *Opt. Lett.*, **18**, 1019-1021.

Davis, A., D. M. Winker, A. Marshak, J. D. Spinhirne, R. F. Cahalan, S. P. Love, S. H. Melfi, and W. J. Wiscombe, 1997: Retrieval of physical and optical cloud thicknesses from space-borne and wide-angle lidar, in *Advances in Atmospheric Remote Sensing with Lidar*. Eds. A. Ansmann, R, Neuber, P. Rairoux, and U. Wadinger, Springer-Verlag, pp. 193-196.

Davis, A. B., R. F. Cahalan, J. D. Spinhirne, M. J. McGill, and S. P. Love, 1999 : Off-beam lidar: An emerging technique in cloud remote sensing based on radiative Green-function theory in the diffusion domain, *Phys. Chem. Earth (B)*, **24**, 757–765.

Davis, A. B., C. Ho, and S. P. Love, 1998: Off-Beam (Multiply-Scattered) Lidar Returns from Stratus, 2: Space-Time Measurements in a Laboratory Simulation, in *19th International Laser Radar Conference Proceedings*, Eds. U. Singh, S. Ismail, and G. Schwemmer, July 6–10, 1998, Annapolis (Md), NASA Center for Aero-Space Information (CASI), pp. 55–58.

Davis, A. B., D. M. Winker, and M. A. Vaughan, 2001: First Retrieval of Boundary-Layer Cloud Properties from Off-Beam/Multiple-Scattering Lidar Data Collected in Space, in *Laser Remote Sensing of the Atmosphere*. Eds. A. Dabas and J. Pelon, École Polytechnique, Palaiseau (France), pp. 35-38.

Love, S. P., A. B. Davis, C. Ho, and C. A. Rohde, 2001: Remote sensing of cloud thickness and liquid water content with Wide-Angle Imaging Lidar," *Atmospheric Research* **59-60**, 295-312.

Priedhorsky, W. C., R. C. Smith, and C. Ho, 1996: Laser ranging and mapping with a photon-counting detector," *Appl. Opt.*, **35**, 441–452.

4. WAIL RETRIEVALS OF CLOUD PROPERTIES

In previous papers (Davis et al. 1997, 1999), we gave detailed theoretical treatments of off-beam lidar in the diffusion regime, both analytical and numerical Monte Carlo modeling. Here we present only a brief summary of the key results relevant to interpreting WAIL data.

At this point in time, we only use two average quantities from the space-time WAIL data: mean in-cloud pathlength $\langle\lambda\rangle$, and root-mean square horizontal displacement $\langle\rho^2\rangle^{1/2}$. In the following, it is only important to know that these two observables have different dependencies on "rescaled" cloud optical depth $(1-g)\tau$ where g is the asymmetry factor of the scattering phase function. Figure 4 shows how the cloud parameters are obtained from the data using the example in Fig. 1.

Apart from merging the datasets from the more- and less off-beam filters in Fig. 1, the only parts of the data analysis that requires human intervention is to manually define cloud-base and the laser impact point in the temporal and spatial domains as well as find the noise-level to subtract.

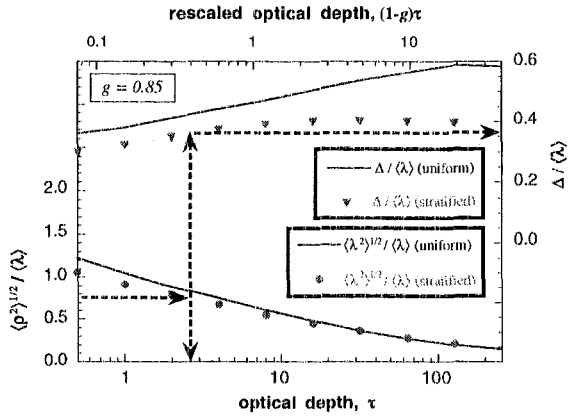

Figure 4: *Retrieval of cloud properties from the data in Fig. 1.* The lower curve shows calculated ratios of two different 2nd-order moments to the 1st-order moment of the pathlength distribution. It is plotted vs. optical depth for a uniform cloud (line) and for a more realistic stratified cloud (symbols) in for ground-based observation. The upper curves are calculated ratios of the cloud thickness to mean pathlength. All computations used an asymmetry factor of $g = 0.85$. Ratio values measured with WAIL (cf. Sect. 2) are indicated by the lower dashed horizontal line, whose intersection with the lower curve gives the optical depth. From there, a vertical line to the upper curve yields the thickness Δ; the mean pathlength was found to be approximately 1.37 km, yielding a physical cloud thickness of 0.52 km.

5. CONCLUSION AND OUTLOOK

Off-beam lidar has advanced rapidly since its inception in the year leading up to Davis et al. (1997). Furthermore, the WAIL project at LANL is not the only one engaged in off-beam lidar development. At NASA-GSFC, Dr. Robert Cahalan has been spearheading the THickness from Off-beam Returns (THOR) project, an airborne design recently deployed for validation at the ARM site (at the same time as WAIL with its new detector), over the same timeframe. Drs. K. F. Evans (U. of Colorado/PAOS) and P. Lawson (Spec, Inc.) are testing an "in-situ" cloud lidar concept based on the same photon diffusion concepts as off-beam lidar. In this case, the aircraft is flying inside the cloud layer rather than far (c. 10 km) above it. As shown by Davis et al. (2001), the Lidar In space Technology Experiment (LITE) on a 1994 shuttle mission was a highly successful, if somewhat inadvertent, off-beam cloud lidar without any spatial resolution, only time; cloud property retrievals are still possible.

We therefore anticipate a bright future for lidar techniques that fully exploit —rather than avoid or mitigate— multiple scattering to probe dense clouds.

REFERENCES

Agnelli, C., A. Cacciani, and M. Fofi, 1975: The magneto-optical filter, *Solar Physics*, **44**, 509-518.

Davis, A., D. M. Winker, A. Marshak, J. D. Spinhirne, R. F. Cahalan, S. P. Love, S. H. Melfi, and W. J. Wiscombe, 1997: Retrieval of physical and optical cloud thicknesses from space-borne and wide-angle lidar, n *Advances in Atmospheric Remote Sensing with Lidar*, Eds. A. Ansmann, R. Neuber, P. Rairoux, and U. Wadinger, Springer-Verlag, pp. 193–196.

Chen, H., C. Y. She, P. Searcy, and E. Korevaar, 1993: Sodium-vapor dispersive Faraday filter, *Opt. Lett.*, **18**, 1019-1021.

Davis, A., D. M. Winker, A. Marshak, J. D. Spinhirne, R. F. Cahalan, S. P. Love, S. H. Melfi, and W. J. Wiscombe, 1997: Retrieval of physical and optical cloud thicknesses from space-borne and wide-angle lidar, in *Advances in Atmospheric Remote Sensing with Lidar*. Eds. A. Ansmann, R, Neuber, P. Rairoux, and U. Wadinger, Springer-Verlag, pp. 193-196.

Davis, A. B., R. F. Cahalan, J. D. Spinhirne, M. J. McGill, and S. P. Love, 1999 : Off-beam lidar: An emerging technique in cloud remote sensing based on radiative Green-function theory in the diffusion domain, *Phys. Chem. Earth (B)*, **24**, 757–765.

Davis, A. B., C. Ho, and S. P. Love, 1998: Off-Beam (Multiply-Scattered) Lidar Returns from Stratus, 2: Space-Time Measurements in a Laboratory Simulation, in *19th International Laser Radar Conference Proceedings*, Eds. U. Singh, S. Ismail, and G. Schwemmer, July 6–10, 1998, Annapolis (Md), NASA Center for Aero-Space Information (CASI), pp. 55–58.

Davis, A. B., D. M. Winker, and M. A. Vaughan, 2001: First Retrieval of Boundary-Layer Cloud Properties from Off-Beam/Multiple-Scattering Lidar Data Collected in Space, in *Laser Remote Sensing of the Atmosphere*. Eds. A. Dabas and J. Pelon, École Polytechnique, Palaiseau (France), pp. 35-38.

Love, S. P., A. B. Davis, C. Ho, and C. A. Rohde, 2001: Remote sensing of cloud thickness and liquid water content with Wide-Angle Imaging Lidar," *Atmospheric Research* **59-60**, 295-312.

Priedhorsky, W. C., R. C. Smith, and C. Ho, 1996: Laser ranging and mapping with a photon-counting detector," *Appl. Opt.*, **35,** 441–452.

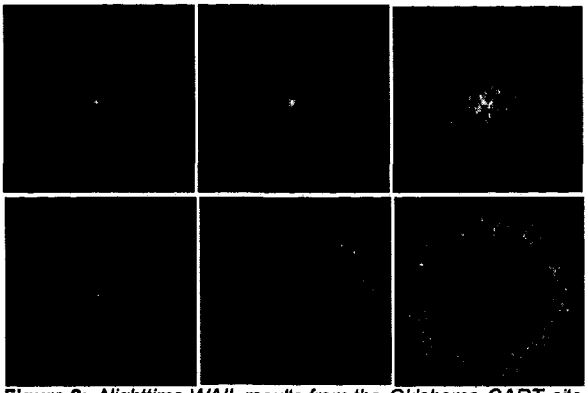

Figure 2: *Nighttime WAIL results from the Oklahoma CART site,* March 24, 2002, using the gated intensified CCD detector system. Top row shows representative WAIL time slices, showing cloud impact and subsequent spreading, using the 536 nm band center interference filter, which passes the center region while suppressing the large angle scattering. Bottom row shows corresponding frames from a data set using the 546 nm filter, which passes returns from the edge of the FOV. Field of view of each frame is 70 degrees. CCD gate width is 50 ns.

Figures 1 and 2 show representative results from the two detector systems Figure 1 shows nighttime results for a multi-layer cloud deck, probed with two different filters on the MCP/CDL detector, one (nominal band center at 540 nm) which strongly suppresses the center spot, and the other (nominal band center at 536 nm) providing a more uniform response across the field. In each case, the spatially integrated return as a function of time (i.e. the temporal Green function) is plotted, along with representative frames of the spatial WAIL "movie," each frame showing the full 60° FOV. Figure 2 shows sample frames from CCD data sets collected at DOE's Southern Great Plains Cloud and Radiation Testbed (CART) site, again with two interference filters, this time 536 nm and 546 nm.

In both cases, we see cloud-base impacts followed by a strong spreading due to multiple scattering in the highest/densest layer. For QuickTime™ movie versions of these and other datasets, see http://nis-www.lanl.gov/~love/clouds.html.

3. TOWARDS A DAYTIME-CAPABLE WAIL

We are presently developing daylight capability for WAIL by means of an ultra-narrow magneto-optic filter coincident with strong solar Fraunhofer absorption lines. This filter uses Faraday rotation in sodium vapor to produce a 90° rotation of the plane of polarization for light propagating along the direction of the applied magnetic field. Placed between crossed polarizers, this results in an extremely narrow transmission band centered at the Na lines (Agnelli et al. 1975). Apart from their extreme narrowness and the convenient coincidence with the Na Fraunhofer lines, their most important feature for WAIL is that, unlike interference filters, their bandpass wavelength is nearly independent of the angle of incidence, at least for small angles. This is because the Faraday rotation is proportional to both the dot product of the direction of propagation and the B-field direct (~cosθ), and to the distance traveled through the Na vapor (~ 1/cosθ), the two angular terms thus canceling. We have built a sodium Faraday filter incorporating internal optics to provide a 60° external field of view while keeping the internal range of angles within the Na vapor cell to less than 20°. Shown in Fig. 3 (left hand side), it uses SmCo permanent magnets to produce a 2700 gauss field inside the Na cell. The expected transmission characteristics, calculated using the model of Chen et al. (1993) are also shown in Fig. 3 (right hand side). Detailed verification of this curve is awaiting completion of the dye laser system that will be used as the transmitter in the daylight WAIL system.

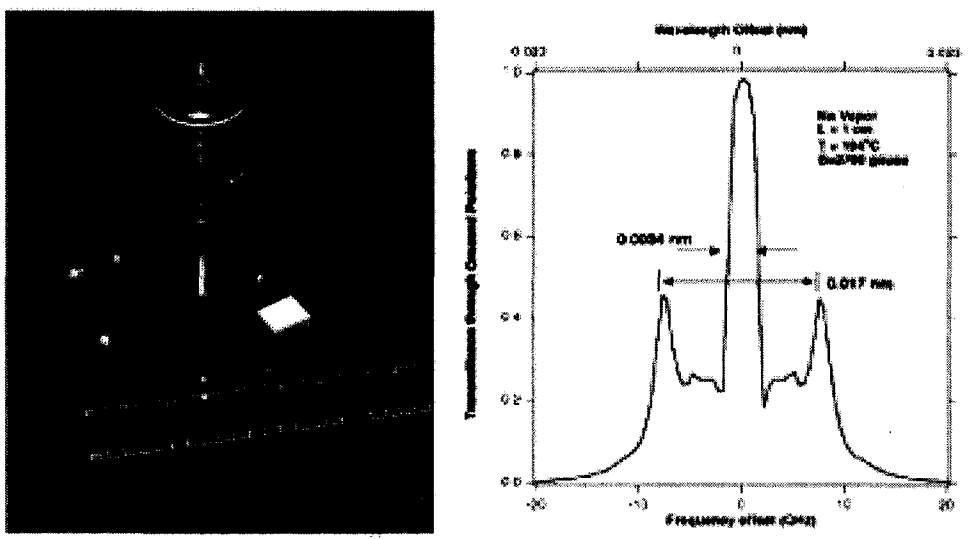

Figure 3: *Wide-angle Na Faraday atomic line filter.* Left: photograph of the assembled filter with one its eight SmCo magnets partially withdrawn. Right: calculated transmittance of the filter; center wavelength is 589 nm.

MCP/CDL. If, instead of a filter centered (at normal incidence) at the laser wavelength, one chooses a somewhat longer nominal filter wavelength, light at large angles of incidence (i.e., coming from the edge of the FOV) will be near the angle-shifted center of the filter passband, while light near normal incidence (i.e., coming from the bright central spot) will be in the wings of the filter passband and be strongly attenuated. The resulting images in this case will show a bright annular region of strong transmission with a dark center.

Our second implementation of the WAIL concept, recently deployed in an experiment at the DOE Atmospheric Radiation Measurements (ARM) program Cloud and Radiation Testbed (CART) site in Oklahoma, makes use of a commercial (Roper Scientific/Princeton Instruments "PI-Max") intensified gated CCD as the receiver. For this 18 mm detector array, we use a lens with 12.5 mm focal-length, resulting in a 70° square field of view. To keep data volumes manageable, we bin the original 512x512 pixel images down to 128x128 pixels.

The gated/intensified CCD detector technology, like the MCP/CDL, uses a micro-channel plate photomultiplier, but there the similarity ends. First, the MCP/CDL has an ultimate time resolution of 100 ps, compared to 2 ns for the CCD system, but this difference is unimportant for cloud measurements where relevant time scales are tens of ns and longer. More important are the differences in the basic modes of operation. Unlike the MCP/CDL system, which time-tags each photon as it arrives, producing raw data consisting of a long stream of time- and space-tagged photon events, the gated CCD system achieves time resolution by electronically gating the intensifier, with gate delay and gate width as adjustable parameters. The MCP/CDL system collects an entire time series for each laser pulse (although only a few photons per pulse can be collected), with good statistics achieved by integrating results for many pulses. The intensified gated CCD, in contrast, collects returns for a single delay time (determined by the gate delay setting), again integrating multiple pulses to achieve good statistics, then advances the gate delay relative to the laser trigger to collect the next "movie frame." There are advantages and disadvantages to both approaches. The CCD can collect many more photons per laser pulse than the MCP/CDL system, the latter being severely constrained by its pulse-timing imaging scheme. Also, the programmable, adjustable gate width of the CCD system allows the exposure time to be adjusted automatically during the course of the measurement, with short exposures for the bright early returns, and longer exposures for the dim high-order scattering. This considerably ameliorates the problems caused by the large dynamic range of the cloud-scattered returns. On the other hand, both systems require total integration times on the order of a minute to collect a complete scattering "movie" with good statistics, and clouds can change on this time scale. The MCP/CDL has the advantage of collecting complete time sequences for each shot, with the result that a time-varying cloud is simply averaged in a straightforward manner in the final multi-pulse integrated data set. But if the cloud changes significantly during measurement with the CCD system, the beginning and end of the time sequence may correspond to very different clouds. Thus with a rapidly varying cloud deck, it is necessary to average many CCD data sets to achieve well-averaged data comparable to that obtained with the MCP/CDL version.

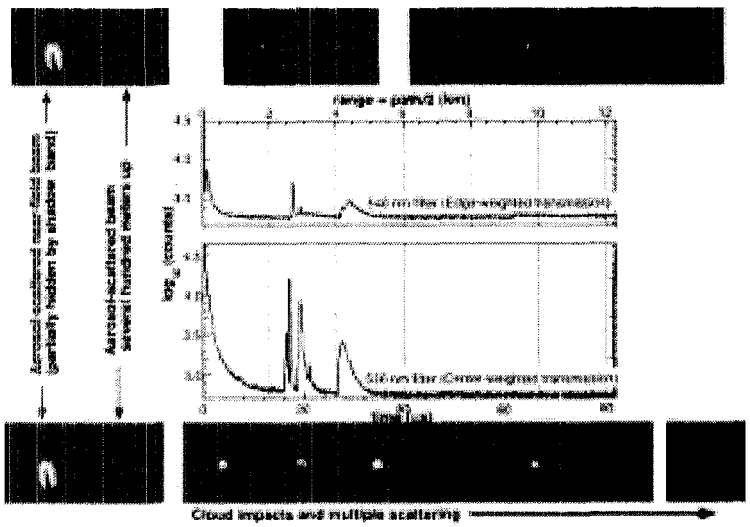

Figure 1: *Nighttime WAIL results using the MCP/CDL detector system.* Shown here are the spatially integrated total return as a function of time (graphs) and a sequence of selected frames from the corresponding WAIL "movies" which show the spatial distribution of the returning light as a function of time. The full-angle FOV is approximately 60°. Two data sets for essentially the same cloud deck are shown, being taken a just few minutes apart. These were obtained with two different filters on the optics, one that emphasizes the large-angle returns (top) and the other emphasizing the center region (bottom). Narrow bandpass interference filters are generally used to reject background light, but also affect the spatial response of the system (see text). Each sequence begins with the Rayleigh/aerosol-scattered beam as it leaves the laser (located off the bottom right side of the FOV); a shadowband blocks the brightest portion of this early return. For these early times, the system is effectively bistatic. Subsequent frames show the aerosol-scattered pulse several hundred meters up, the initial impact on the cloud deck, and subsequent spreading due to multiple scattering. Notice the multiple layers in the lower (smaller-angle) plot.

J5.3 ACTIVE PROBING OF CLOUD THICKNESS AND OPTICAL DEPTH USING WIDE-ANGLE IMAGING LIDAR

Steven P. Love,* Anthony B. Davis, Charles A. Rohde, Larry Tellier, Cheng Ho
Space and Remote Sensing Sciences Group (NIS-2), Los Alamos National Laboratory

1. INTRODUCTION AND OVERVIEW

At most optical wavelengths, laser light in a cloud lidar experiment is not absorbed but merely scattered out of the beam, eventually escaping the cloud via multiple scattering. There is much information available in this light scattered far from the input beam, information ignored by traditional "on-beam" lidar. Monitoring these off-beam returns in a fully space- and time-resolved manner is the essence of our unique instrument, Wide Angle Imaging Lidar (WAIL). In effect, WAIL produces wide-field (60° full-angle) "movies" of the scattering process and records the cloud's radiative Green functions. A direct data product of WAIL is the distribution of photon path lengths resulting from multiple scattering in the cloud. Following insights from diffusion theory, we can use the measured Green functions to infer the physical thickness and optical depth of the cloud layer. WAIL is notable in that it is applicable to optically thick clouds, a regime in which traditional lidar is reduced to ceilometry.

Section 2 covers the up-to-date evolution of the nighttime WAIL instrument at LANL. Section 3 reports our progress towards daytime capability for WAIL, an important extension to full diurnal cycle monitoring by means of an ultra-narrow magneto-optic atomic line filter. Section 4 describes briefly how the important cloud properties can be inferred from WAIL signals.

2. EVOLUTION OF WAIL INSTRUMENTATION

The basic idea of WAIL is to send a short-pulse, narrow-beam laser into a cloud, and record, as a function of both space and time, the intensity of the returning light over a wide field of view (Davis et al. 1997, 1999). In essence, one wants to take a "movie" of the propagation of the multiply-scattered light. The first realization of such a fully imaging WAIL instrument (Love et al., 2001) relies on unique imaging detector technology developed at Los Alamos National Laboratory, Priedhorsky et al.'s (1996) Micro-channel Plate/Crossed Delay Line (MCP/CDL) detector coupled with high-speed pulse absolute timing electronics. The MCP/CDL technology features photon-counting sensitivity, effectively up to ~1500^2 pixels, and ultra-high time resolution (100 ps). It consists of the MCP/CDL detector — a photo-cathode coated vacuum tube, intensified by micro-channel plates, read out by a crossed delay line anode — together with fast pulse-timing electronics. Each photo-electron is intensified by a factor of 10^7, with positional information preserved, by the MCP. The electron cloud is collected by helically wound delay lines, producing in each line two counter-propagating current pulses which emerge from the ends. By measuring the arrival times of the pulses at the ends of the delay lines, the position of the original photon event is determined; with two orthogonal delay lines, both the *x*- and *y*- coordinates are determined. This unique strategy for extracting spatial information distinguishes the MCP/CDL from other sensitive imagers such as gated/intensified CCDs. As an early test, we exploited the extremely high time resolution (100 ps corresponds to a path-length of only 3 cm) to perform laboratory-scale simulations of off-beam lidar, where the "cloud" was an aquarium filled with a scattering liquid suspension (Davis et al. 1998).

This detector is not only capable of performing at very low light-levels, but actually requires them: too high a count rate (>5×10^6/sec over the entire detector) confuses the timing-based imaging scheme. This count rate limit demands a high laser repetition rate and averaging over many pulses. Repetition rate around 5–15 kHz is ideal, permitting maximal pulse averaging while avoiding the return from one pulse overlapping with the next. The MCP's spectral response makes a 532 nm frequency-doubled Nd:YAG laser a good choice. Our laser produces 0.2–0.5 mJ/pulse at a variable rep rate (12 kHz is typical for us), with pulse widths ranging from 30 ns to 50 ns depending on operating conditions. The laser is triggered by a master clock, which also provides the timing reference for the detector system electronics.

This nighttime WAIL implementation uses a standard medium-format camera lens with a 35 mm focal length to feed the detector, thus obtaining a full-angle FOV of 60°. This wide angle is needed for ground-based measurements, because the high-order scattering tail of interest here extends up to a kilometer from the beam, a distance comparable to the typical range to the cloud base. One challenge in this experiment is the large dynamic range, several orders of magnitude, between the initial return (the traditional on-beam lidar signal) and the multiply scattered returns from locations at very large displacements from the beam. The faint large-displacement returns require a band-pass filter, ≈10 nm wide for nighttime work, to reject as much background light as possible. The use of interference filters presents an apparent problem, given the wide field of view, since, as is well known, the band center for standard interference filters varies strongly with angle of incidence. Over the 30° half-angle range of our system, the passband center wavelength shifts nearly 15 nm to shorter wavelengths as one moves from the center to the edge of the field. This angular sensitivity, however, can be put to use to partially cancel the strong center-to-edge gradient intrinsic to cloud returns but challenging to any detector system, particularly to our

* *Corresponding author:* Steven P. Love, LANL, MS C323, Los Alamos, NM 87545; 505 667-0067; fax 505 667-3815; email: splove@lanl.gov.